TSSA Journal of Tomography System & Sensors Application Vol. 9, Issue 1, 2026
www.tssa.com.my e-ISSN: 636-9133

Initial Study of Magnetic Induction Tomography for Crack Detection of Composite Pipe

Arif Luqman Azmi[1], Yasmin Abdul Wahab[1*], Nurul 'Ain Nadzri[1], Mohd Mawardi Saari[1], Suzanna Ridzuan Aw[2], Siti Zarina Muji[3], Ruzairi Abdul Rahim[4], Sia Yee Yu[5]

[1]Faculty of Electrical & Electronics Engineering Technology, Universiti Malaysia Pahang Al- Sultan Abdullah, 26600 Pekan, Pahang, Malaysia
[2]Faculty of Electrical & Automation Engineering Technology, Terengganu Advance Technical Institute University College (TATiUC), Jalan Panchor, Telok Kalong, 24000 Kemaman, Terengganu, Malaysia
[3]Faculty of Electrical and Electronic Engineering, Universiti Tun Hussein Onn Malaysia, 86400 Parit Raja, Batu Pahat,Johor, Malaysia
[4]Process Tomography Research Group and Instrumentation (PROTOM-i), Faculty of Electrical Engineering, Universiti Teknologi Malaysia, 81310 UTM Skudai, Johor, Malaysia
[5]LOGO Solution Sdn. Bhd., suite 0525, Level 5, Wisma SP Setia, Jalan Indah 15, Bukit Indah, 79100 Iskandar Puteri Johor Malaysia

Corresponding author* email: yasmin@umpsa.edu.my
Available online 01 March 2026

ABSTRACT

This study investigates the feasibility of Magnetic Induction Tomography (MIT) as a non-invasive method for detecting cracks in glass fiber-reinforced composite pipes, which are increasingly used in the oil and gas industry. An MIT system was modeled in COMSOL Multiphysics using eight copper coils arranged circumferentially around the pipe. Crack scenarios with varying opening angles, positions, and numbers were simulated. Sensor data were processed in MATLAB using a Linear Back Projection (LBP) algorithm to reconstruct tomographic images. The Mean Structural Similarity Index (MSSIM) values were generally below 0.1, with the highest value observed for a single crack with a 20° opening angle. The results indicate that MIT can detect and localize cracks in composite pipes, demonstrating the method's potential for this application.

Keywords: magnetic induction tomography, composite pipe, crack detection, image reconstruction, LBP

1. Introduction

The oil and gas industry is shifting from steel to composite pipes due to the latter's improved corrosion and erosion resistance. However, most existing MIT research has focused on steel pipes [1], leaving a gap regarding its feasibility for composite materials. Key challenges include establishing the sensitivity of MIT to defects in low-conductivity, low-permeability composites, and designing suitable sensor configurations for such applications. This work aims to assess the feasibility of applying MIT to composite pipes through simulation and image reconstruction, and to evaluate the detectability of cracks with varying sizes, positions, and counts [2], [3]. Despite these advantages, the nondestructive evaluation of composite pipelines remains challenging due to their low electrical conductivity and anisotropic layups, which reduce electromagnetic contrast and complicate defect characterization using contact-based methods. Given MIT's contactless operation and ability to sense through coatings and insulation, it is a promising candidate for rapid screening of composite pipes in situ, complementing conventional techniques by localizing conductivity perturbations associated with cracks. Building on prior MIT studies that established feasibility on conductive targets and small-scale systems, this work focuses on composite-specific detectability and localization trends to inform coil configuration, excitation strategy, and reconstruction choices under low-contrast conditions.

2. Magnetic Induction Tomography

Magnetic Induction Tomography (MIT) uses eddy currents to image an object's passive electrical properties (PEP), namely conductivity (σ), permeability (μ), and permittivity (ε) [4]. The approach is non-invasive, non-destructive, and contactless. MIT has been applied across domains such as geophysics [1] , medical imaging [5][6] and non-destructive testing [7]. It also sees use in process industries [8][9]. In MIT, an excitation coil generates a time-varying magnetic field, including eddy currents in the object [10].

Figure 1 illustrates the principle of MIT, showing induced eddy currents and the resulting field perturbations.

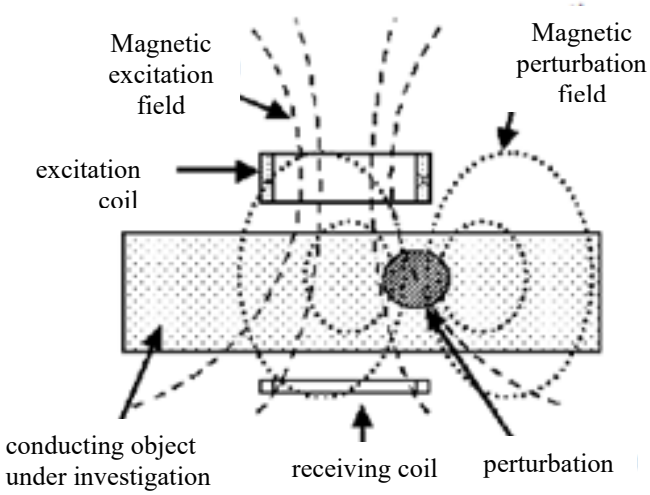

Figure 1. Principle of MIT[10]

The magnetic field intensity can be described by Ampère's circuital law, which states that the line integral of the magnetic field strength H around a closed path equals the enclosed current I:

$$\int H.dl = I \quad (1)$$

Where
H= magnetic field strength (A/m)
I=Current(A)
dl=differential length of element along the path of integration

MIT systems typically employ multiple coils as transmitters and receivers to generate and sense field perturbations caused by defects or inhomogeneities. While applications to conductive metals are established, composite pipes—characterized by lower μ and σ—remain underexplored.

3. Methodology

We modeled a two-dimensional MIT system for composite pipe inspection in COMSOL Multiphysics and performed image reconstruction in MATLAB using the LBP algorithm. Figure 2 presents the workflow, from electromagnetic simulation to tomogram generation.

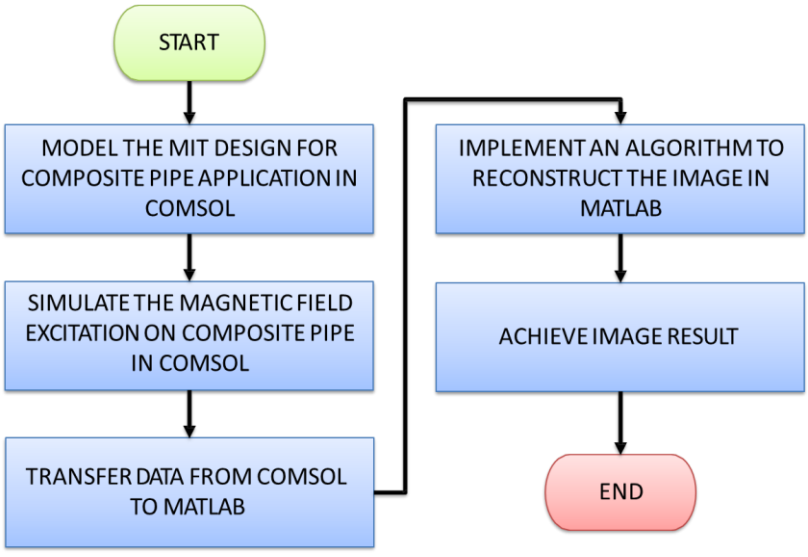

Figure 2. Basic flow process in this simulation study

The sensing region comprises eight copper coils arranged around a glass fiber-reinforced polymer (GFRP) pipe with 110 mm inner diameter and 3.8 mm wall thickness (Figure 3). GFRP was selected due to its high specific strength and stiffness, and excellent corrosion and erosion resistance, making it suitable for oil and gas applications[11]. Coils are divided into excitation and sensing roles and are cycled to cover all transmit–receive combinations [12][13][17]. Coil parameters:

The properties and dimension of the coils are as follow:

- Made of copper
- Exciting coils and sensing coils
- Width = 0.01m
- Length = 0.08m
- Excitation current = 10mA
- Number of turns in excitation coil = 4

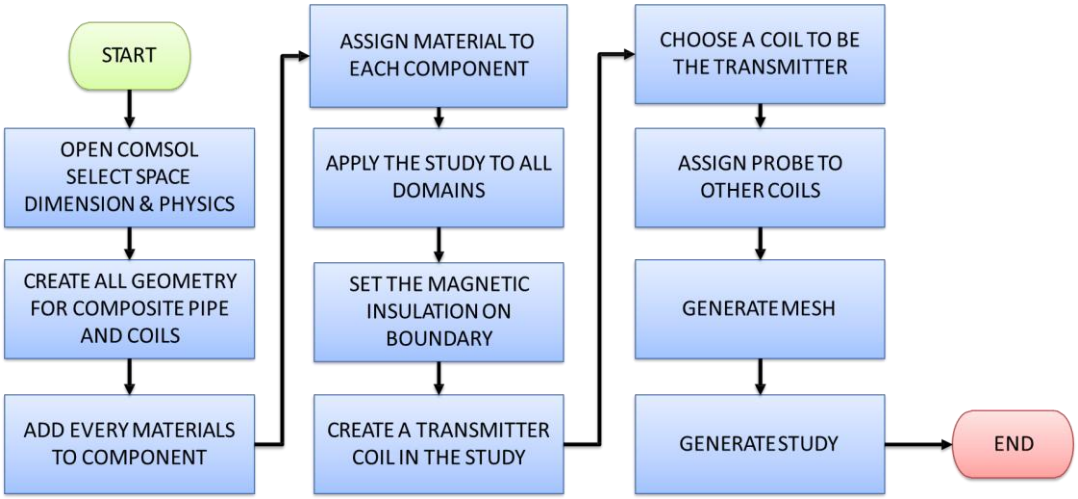

Figure 3. Basic flow process in COMSOL Multiphysics

Each domain was assigned materials consistent with representative properties (Table 1). Ampère's Law physics was applied to all domains. A magnetic insulation boundary was set at the exterior to confine fields within the model domain. Excitation was applied to the active transmitter coil (e.g., Tx1 in Figure 4), while the remaining coils acted as receivers.

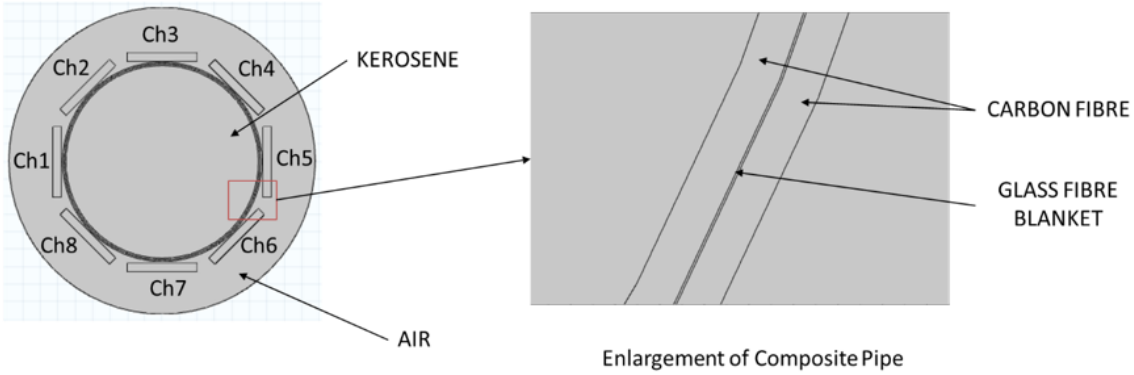

Figure 4. Geometry design of composite pipe and sensing zone

Table 1. Material properties

Material	Electrical Conductivity (S/m)	Relative Permeability	Relative Permittivity
Kerosene	50×10^{-12}	2.1	1.8
Carbon Fiber	10	100	1
Glass Fiber Blanket	10×10^{-15}	38	10
Copper	5.998×10^{7}	1	1
Air	10×10^{-12}	1	1.0006

In magnetic physics, several key elements are considered, including Ampere's Law, magnetic insulation, initial values, and the coil designated as the transmitter. Firstly, the Ampere's law physics was assigned to all domain in the MIT system which is crucial to ensure all the domains comply with the Ampere's law. The magnetic insulation was then assigned to the outside circle, which stands for the MIT system's surroundings. Its purpose is to ensure that the transmitter's current excitation stays inside the intended model only. The physical use was for a coil, which has four turns and excited a 10mA current. Figure 5 shows the example when channel 1 becomes as the transmitter. Each of the coils involved in this model was alternately change their roles as transmitter and receiver channel till complete cycle [14]. Meshing used a "finer" setting to resolve field gradients (Figure 6).

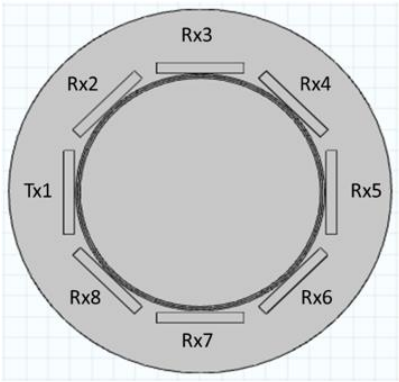

Figure 5. Example channel 1 as transmitter, Tx1

We investigated three variables: crack opening angle (20°, 45°, and 90°), angular position (e.g., right-top, left-top, left-bottom), and number of cracks (single, double, triple). Field contour and sensor responses were exported to MATLAB. LBP was used to reconstruct images of the sensing region. Reconstruction quality was evaluated using MSSIM, comparing reconstructed tomograms to corresponding reference images.

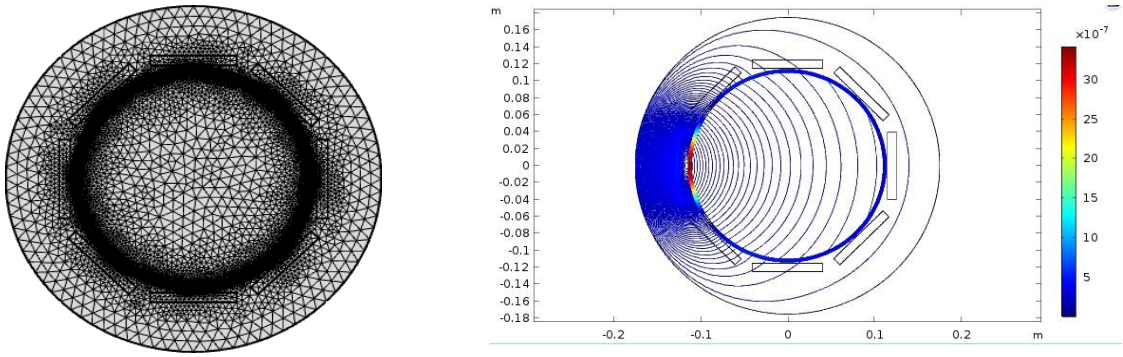

(a) (b)

Figure 6. (a) Finer mesh and (b) example of magnetic field contour (no crack)

4. Results and Discussion

Table 2 shows the different tested conditions. For a single crack at the right-top position, increasing opening angle from 20° to 90° produced progressively larger local distortions, indicating increased detectability. Changing crack position (left-top, left-bottom) consistently localized the field perturbation near the defect, indicating angular coverage is adequate for localization. Double and triple-crack configurations produced multiple disturbed regions and more complex field patterns, reflecting the superposition of defect effects.

LBP reconstructions captured defect locations for single-crack scenarios, though image blur increased with larger opening angles, consistent with reduced MSSIM. For single cracks at the right-top position, MSSIM decreased from 0.0820 (20°) to 0.0794 (90°). Left-top and left-bottom single-crack cases yielded MSSIM values of 0.0807 and 0.0847, respectively, with the left-bottom case slightly better. Double and triple cracks were identifiable, though images were blurrier (MSSIM ≈ 0.0780 and 0.0802). Overall MSSIM values below 0.1 indicate modest structural similarity to ground truth, which is expected given LBP's smoothing and the low-contrast nature of composites. These findings motivate future use of advanced reconstruction (e.g., Tikhonov, TV, or model-based nonlinear methods) to improve fidelity.

Figure 7 compares magnetic field magnitudes for homogeneous (no crack) and 20° size of cracked cases. The single cracked case was taken from the 20° size of cracked at the top right position. The homogeneous pipe shows a near-uniform profile, whereas crack scenarios introduce distinct deviations, with magnitude increasing alongside crack count. These trends suggest that the system can potentially classify the presence and number of cracks based on receiver patterns.

The composite's low conductivity and permeability reduce induced currents compared to metals, lowering signal contrast and contributing to lower MSSIM. The 2D approximation simplifies coil–pipe coupling and neglects axial effects. Despite these limitations, the results demonstrate consistent localization and sensitivity trends, supporting the feasibility of MIT for composite pipe crack detection.

Table 2. Different position and size of crack

Position and size of crack	Geometry	Contour	Reference image	Tomogram	MSSIM
Right top 20°	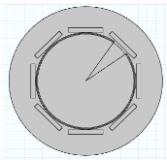	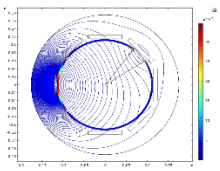	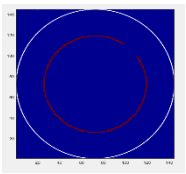	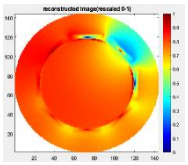	0.0820
Right top 45°	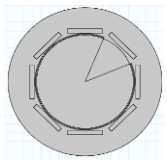	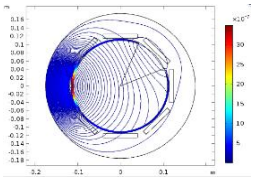	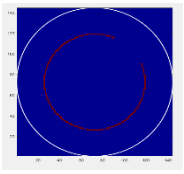	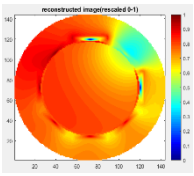	0.0809
Right top 90°	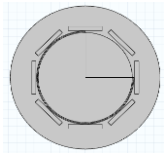	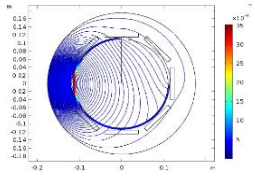	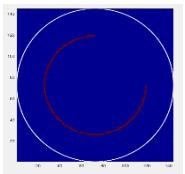	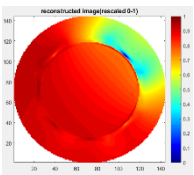	0.0794
Left top 20°	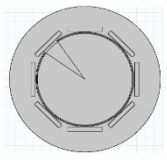	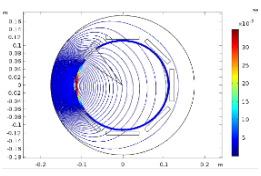	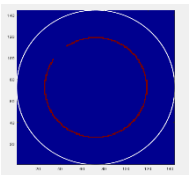	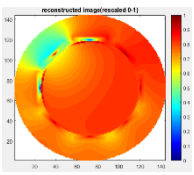	0.0807

Left bottom 20°	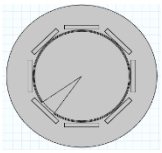	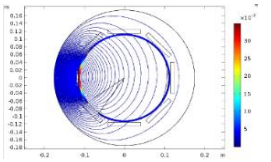	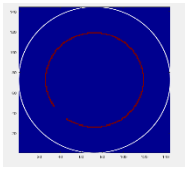	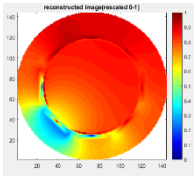	0.0847
Double crack of 20°	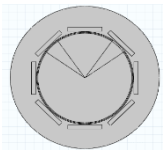	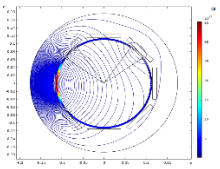	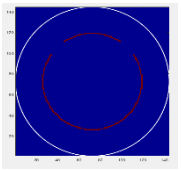	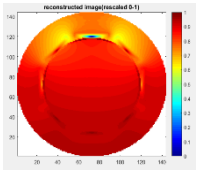	0.0780
Triple crack of 20°	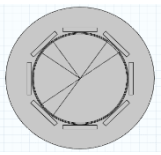	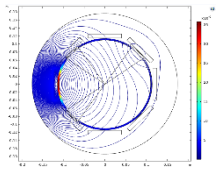	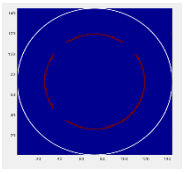	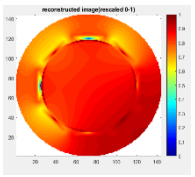	0.0802

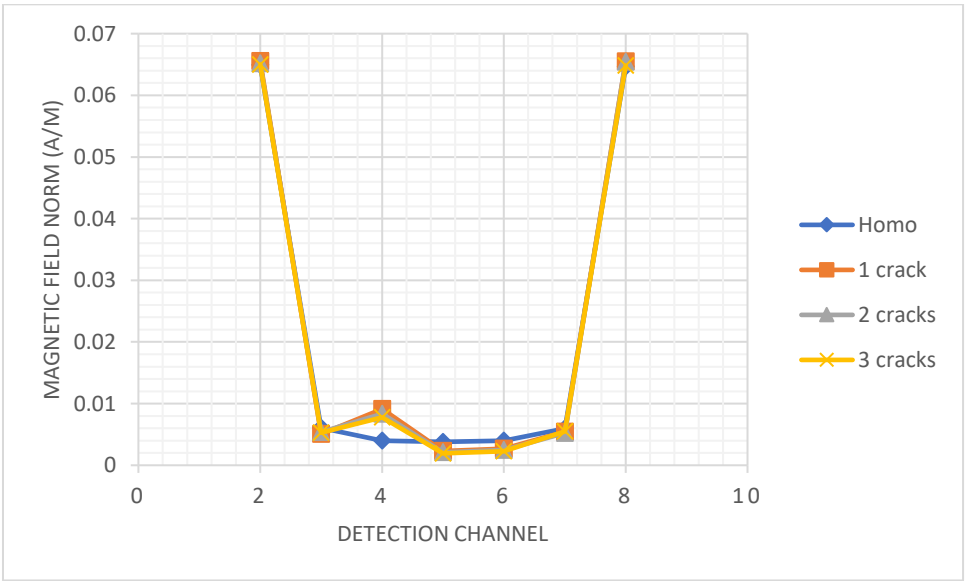

Figure 7. Magnetic field comparison between homogenous and different number of cracks

5. Conclusions

In conclusion, we demonstrated the feasibility of MIT for detecting and localizing cracks in GFRP composite pipes via 2D COMSOL simulations and LBP reconstruction. Field contour and tomograms consistently reflected defect presence, position, and size. While MSSIM values were modest (<0.1), they are consistent with LBP on low-contrast media. Future work will focus on improved reconstruction algorithms (e.g., Tikhonov regularization, sparsity constraints, or learned priors), 3D modeling, hardware validation, and sensitivity optimization (coil geometry, frequency selection, and excitation strategies).

Acknowledgment

The authors would like to thank the Universiti Malaysia Pahang Al-Sultan Abdullah for laboratory facilities.

References

[1] R. Guilizzoni, G. Finch, and S. Harmon, "Subsurface Corrosion Detection in Industrial Steel Structures," *IEEE Magnetics Letters*, vol. 10, 2019, doi: 10.1109/LMAG.2019.2948808.

[2] N. Ishak, C. K. Lee, and S. Z. Mohd Muji, "A simulation magnetic induction tomography (MIT) for agarwood using COMSOL Multiphysics," *International Journal of Engineering and Advanced Technology*, vol. 10, no. 3, pp. 67–71, 2021, doi: 10.35940/ijeat.c2174.0210321.

[3] M. S. B. Mansor, R. A. Rahim, Z. Zakaria, N. M. N. Ayob, Y. M. Yunus, and A. Ahmad, "Small Scale Non-Invasive Imaging Using Magnetic Induction Tomography - Hardware Design," *International Journal of Integrated Engineering*, vol. 12, no. 8, pp. 20–30, 2020, doi: 10.30880/ijie.2020.12.08.003.

[4] Q. Du, X. Sun, L. Ke, C. Wang, and Y. Liu, "Study on magnetic induction tomography system using magnetic focusing coils," in *6th International Conference on Biological Information and Biomedical Engineering*, 2022, pp. 175–179.

[5] J. Liu, L. Chen, H. Xiong, and Y. Han, "Review of microwave imaging algorithms for stroke detection," *Medical and Biological Engineering and Computing*, vol. 61, no. 10, pp. 2497–2510, 2023, doi: 10.1007/s11517-023-02848-5.

[6] Z. Xiao, C. Tan, and F. Dong, "3-D Hemorrhage Imaging by Cambered Magnetic Induction Tomography," *IEEE Transactions on Instrumentation and Measurement*, vol. 68, no. 7, pp. 2460–2468, 2019, doi: 10.1109/TIM.2019.2900779.

[7] S. Y. A. Fatah *et al.*, "Advancements in Underground Object Detection: Exploring Emerging Techniques and Technologies," *2024 International Telecommunications Conference, ITC-Egypt 2024*, pp. 852–857, 2024, doi: 10.1109/ITC-Egypt61547.2024.10620483.

[8] M. Soleimani *et al.*, "In situ steel solidification imaging in continuous casting using magnetic induction tomography," *Measurement Science and Technology*, vol. 31, no. 6, 2020, doi: 10.1088/1361-6501/ab6f30.

[9] Y. Zhu, S. C. Wei, Y. Liang, Y. J. Wang, and Y. C. Dong, "Research on ultrasonic testing and image preprocessing method of remanufactured oil pipe inner wall," *Proceedings of 2017 IEEE Far East NDT New Technology and Application Forum, FENDT 2017*, pp. 23–25, 2018, doi: 10.1109/FENDT.2017.8584582.

[10] M. S. B. Mansor *et al.*, "Magnetic induction tomography: A brief review," *Jurnal Teknologi*, vol. 73, no. 3, pp. 91–95, 2015, doi: 10.11113/jt.v73.4252.

[11] T. A. Sebaey, "Design of oil and gas composite pipes for energy production," *Energy Procedia*, vol. 162, pp. 146–155, 2019, doi: 10.1016/j.egypro.2019.04.016.

[12] F. N. Adiputri, E. N. Prasetiani, Rohmadi, A. Saputra, I. Muttakin, and W. P. Taruno, "Simulation of Magnetic Induction Tomography Sensor with 8-Coils Solenoid and Planar," *Proceedings of 2017 5th International Conference on Instrumentation, Communications, Information Technology, and Biomedical Engineering, ICICI-BME 2017*, no. November, pp. 236–240, 2018, doi: 10.1109/ICICI-BME.2017.8537753.

[13] G. Xiaoting, S. Yunpeng, S. Huadong, X. Chunfeng, Z. Haibo, and W. Yunan, "Design and application of magnetoelectric composite heterogeneous field multi-function sensor," *2019 14th IEEE International Conference on Electronic Measurement and Instruments, ICEMI 2019*, pp. 880–885, 2019, doi: 10.1109/ICEMI46757.2019.9101724.

[14] Y. Chen, C. Tan, and F. Dong, "Excitation Strategy Analysis of Magnetuc Indusction Tomography for Intracranial Hemorrhage Detection," in *39th Chinese Control Conference*, 2020, pp. 2780–2785.